Investigation Of Heat Transfer Phenomena And Natural Flow Behavior Around A Heated Square Cylinder Placed In A Cooled Elliptical Enclosure

Dr. Sattar J. Habeeb*

Received on:11/3/2009
Accepted on:5/11/2009

Abstract

In this paper, a numerical study of the effect of a hot square cylinder placed on a cooled elliptical enclosure of a laminar natural convection was carried out. This problem is solved by using the partial differential equations, which are the stream vorticity formulation for the flow and heat transfer in curvilinear coordinates. An elliptical function is used, which makes the coordinate transformation from the physical domain to the computational domain be set up by an analytical expression. About 48 tests are performed for different ratios of the geometry such as, $a/b = 1.5, 2., 3$, $l/b = 0.25, 0.5$, and Rayleigh number from 10^3 to 10^6, for two position of the major axis of the elliptical enclosure, horizontal (HEE) and vertical (VEE). The results obtained in the form of velocity vectors, streamlines, isotherms, and Nusselt number. The results show that, the increase of the major axis of the enclosure (a/b ratio) leads to increase the average Nusselt number and decrease the flow strength for all Rayleigh numbers. Moreover, for $Ra \leq 10^4$, there are a little difference in the results of Nu_{ave} for all a/b and l/b ratios, but if Ra increases, the change in the results is clear and large.

Keywords: natural convection, elliptical enclosure, complex geometry.

بحث ظاهرة انتقال الحرارة وتصرف الجريان الطبيعي حول اسطوانة مسخنة مربعة الشكل موضوعة في حيز مبرد ذا شكل قطع ناقص

الخلاصة

في هذا البحث تم أجراء دراسة عددية لتأثير وجود أسطوانة ساخنة مربعة الشكل موضوعة داخل تجويف مبرد ذا شكل قطع ناقص على أنتقال الحرارة بالحمل الطبيعي. المسألة حُلت بأستخدام المعادلات التفاضلية الجزئية الخاصة بالجريان وأنتقال الحرارة بصيغة دالة الأنسياب-الدوامية وبأحداثيات مطابقة الجسم. تم أستخدام دالة القطع الناقص لتحويل نظام الاحداثيات الفيزياوي الى نظام الاحداثيات الحسابي بواسطة الآشتقاق الرياضي, الدراسة شملت 48 حالة مدروسة لنسب مختلفة من متغيرات الشكل الهندسي للحيز المدروس, مثل $a/b = 1.5, 2., 3$, $l/b = 0.25, 0.5$, و مدى لرقم رايلي من 10^3 الى 10^6 لحالتين لموضع المحور الكبير للحيز (القطع الناقص) أفقيا HEE وعموديا VEE. أستعرضت النتائج بواسطة متجهات السرع, خطوط الأنسياب, خطوط ثبوت درجات الحرارة, ورقم ناسلت. النتائج الرئيسية أظهرت بأن زيادة طول المحور الكبير للحيز (النسبة a/b) تؤدي الى زيادة بقيمة متوسط رقم ناسلت وأنخفاض بشدة الجريان لكل مدى رقم رايلي. بالاضافة الى أن في حالة $Ra \leq 10^4$, هنالك أختلاف طفيف للنتائج الخاصة Nu_{ave} لكل نسب a/b , و l/b , لكن في حالة زيادة رقم رايلي عن ذلك يكون الأختلاف بالنتائج واضح وكبير.

* **Mechanical Engineering Department, University of Technology / Baghdad**

https://doi.org/10.30684/etj.28.4.6
2412-0758/University of Technology-Iraq, Baghdad, Iraq

Introduction

Flow and heat transfer in an elliptical enclosure are of practical important in engineering applications and involved in many industrial systems. Applications of natural convection include solar collector receivers, transmission cable cooling system heat exchangers, nuclear and chemical reactors, aircraft cabin insulation and thermal storage system. In engineering applications, the geometries that arise however are more complicated than a simple enclosure filled with a convective fluid. The geometric configuration of interest is with the presence of bodies' embodied within the enclosure **[1, 2]**.

Roychowdhury et. al. [3] analyzed the natural convective flow and heat transfer features for a heated cylinder kept in a square enclosure with different thermal boundary conditions.

Asan [4] numerically studied two-dimensional natural convection in an annulus between two isothermal concentric square ducts and obtained solutions up to a Rayleigh number of 10^6. The results showed that dimension ratio and Rayleigh number have a profound influence on the temperature and flow fields. **Kumar De and Dalal [5]** considered the problem of natural convection around a titled heated horizontal square cylinder placed inside an enclosure in the range of $10^3 \leq Ra \leq 10^6$. Effects of the enclosure geometry have been assessing using three different aspect ratios placing the square cylinder at different heights from the bottom. As a result, they found that, the uniform wall temperature heating is quantitatively different from the uniform wall heat flux heating. The flow pattern and thermal stratification were modified if the aspect ratio was varied. Overall heat transfer also changes as a function of the aspect ratio.

Kim et. al. [6] investigated numerically the characteristics of two dimensional natural convection problems in a cooled square enclosure with an inner heated circular cylinder. The immersed boundary method was implemented in a second-order accurate finite volume method to simulate the flow and heat transfer over an inner circular cylinder in the Cartesian coordinates. A detailed analysis for the distribution of streamlines, isothermals and Nusselt numbers were carried out to investigate the effect of the locations of the heated inner cylinder on the fluid flow and heat transfer in the cooled square enclosure for different Rayleigh number in the rang $10^3 \leq Ra \leq 10^6$.

Cesini et. al. [7] performed the numerical and experimental analysis of natural convection from a horizontal cylinder enclosed in a rectangular cavity. The influence of the cavity aspect ratio and the Rayleigh number on the distribution of temperature and Nusselt number was investigated. As a result, the average heat transfer coefficients increases with increasing Rayleigh number.

Moukalled and Acharya [8] and Shu and Zhu [9] studied the change of the thermo-flow field between the low temperature outer square enclosure and high temperature inner circular cylinder according to the radius of the inner cylinder. They considered three different aspect ratios of the cylinder radios to the enclosure height in the range of $10^4 \leq Ra \leq 10^7$, showed that, at a constant enclosure aspect ratio, the total heat transfer increase with increasing Rayleigh number. When the Rayleigh number is constant, the convection contribution to the total heat transfer decrease with an increasing aspect ratio value. **Shu and Zhu [9]** obtained the numerical result, for Rayleigh numbers ranging from 10^4 to 10^6 and aspect ratios (as a pervious reference) between 1.67 and 5. It was found that, both the aspect ratio and Rayleigh number are critical to the patterns of flow and thermal fields. In addition, they suggested that a critical aspect ratio might exist at high Rayleigh number to distinguish the flow and thermal patterns. **Tasnim and Mahmud [10]** studied numerically the buoyancy induced flow and heat transfer characteristics inside an inclined L-shape enclosure. Results presented in the form of the average Nusselt number for a range of inclination angle 0^o-360^o, Rayleigh number 1-10^5 and aspect ratio 0.1-0.5. **Zhu et. al. [11]** studied the natural convection heat transfer between two horizontal, elliptical cylinders using the differential quatrature (QD) method. It was found that, the position of the major axis of the inner ellipse takes effect on the streamlines and very little effect on the average Nusselt number.

However, there is little information about natural convection processes when a heated square cylinder exists within a cooled elliptical enclosure, for two cases, horizontal elliptical enclosure (HEE) and vertical elliptical enclosure (VEE). The purpose of the present study is to examine how the geometric parameters, a/b, and l/b of the enclosure affects the natural convection phenomena for different Rayleigh numbers.

Problem Specification

A schematic of the system considered in the present study for two cases, horizontal elliptical enclosure (HEE) and vertical elliptical enclosure (VEE) as shown in **figure (1)**. The system consists of an elliptical enclosure with half major axis length a and half minor axis length b, within which a square cylinder with a side length l is located at the centerline of the elliptical enclosure. The walls of the square cylinder kept at constant high temperature T_h whereas the wall of the elliptical enclosure was kept at constant low temperature T_c . In this study, assumed that, the radiation effects are negligible, and the fluid properties are constant except for the density in the buoyancy term, which follows the boussinesq approximation. As the square cylinder and the elliptical enclosure are long enough, so the flow is consider being steady, laminar and two dimensions. The enclosure filled with air and Pr=0.71.

The dimensionless governing equation for the problem is written in the stream – vorticity formulation as:

$$\nabla^2 \cdot y = -w$$
$$w_t + y_y \cdot w_x + y_x \cdot w_y = \Pr \cdot \nabla^2 \cdot w + \Pr \cdot Ra \cdot T_x \quad (1)$$
$$T_t + y_y \cdot T_x + y_x \cdot T_y = \nabla^2 \cdot T$$

Hence, introducing the following non-dimensional variables:

$\mathrm{Ra}=(gb^*(T_h - T_c)l^3/na^*)$,

$\Pr = n/a^*$

$x = x^*/l \;, y = y^*/l \;, u = u^*/(a^*/l)$

$v = v^*/(a^*/l), w = w^* \cdot l/u^*, y = y^*/(u^* \cdot l)$

$T = (t - t_c)/(t - t_c), w = \partial v/\partial x - \partial u/\partial y$

$u = \partial y/\partial y, v = -\partial y/\partial x$

Then using general curvilinear coordinates $x=x(x,h)$, $y=y(x,h)$, the set of non-dimensional transformed equation are [9]:

$$A \cdot y_{xx} + 2B \cdot y_{xh} + C \cdot y_{hh} + G \cdot y_h + H \cdot y_x = -J \cdot w \quad \ldots(2)$$

$$w_t + y_h \cdot w_x - y_x \cdot w_h = \Pr \cdot \begin{bmatrix} A \cdot w_{xx} + 2B \cdot w_{xh} \\ + C \cdot w_{hh} + G \cdot w_h \\ + H \cdot w_x \end{bmatrix} + \Pr \cdot Ra \cdot \left[y_h \cdot T_x - y_x \cdot T_h \right] \quad (3)$$

$$T_t + y_h \cdot T_x - y_x \cdot T_h = \begin{bmatrix} A \cdot T_{xx} + 2B \cdot T_{xh} \\ + C \cdot T_{hh} + G \cdot T_h \\ + H \cdot T_x \end{bmatrix} \quad (4)$$

Where

$a = x_h^2 + y_h^2$, $g = x_x^2 + y_x^2$

$J = x_x y_h - y_x x_h$, $s = x_x x_h + y_x y_h$

$A = a/J$, $B = -s/J$, $C = g/J$

$G = B_x + C_h$, $H = A_x + B_h$

Grid Generation

In this study, an analytical expression could derive for the coordinate transformation from the physical domain to the computational domain; all-geometrical parameters could computed exactly. The super elliptic function could be written as [9]:

$$\left(\frac{x}{a}\right)^{2n} + \left(\frac{y}{b}\right)^{2n} = 1. \quad \ldots (5)$$

Where a and b are half of the elliptic lengths axis's in the x and y direction respectively, n a positive integer. So for this study could be expressed as:

For inner square cylinder

$a = b = l$ *and* $n \geq 50$

For outer elliptical enclosure

$a \neq b$ $(a = 1.5b, 2b, 3b)$ *and* $n = 1$

The coordinate's transformation for the present problem can be exactly setup, which is written as:

$$x = -\sin(x) \cdot \left[r_i + (r_o - r_i) \cdot h \right] \ldots(6)$$
$$y = \cos(x) \cdot \left[r_i + (r_o - r_i) \cdot h \right] \ldots(7)$$

Where r_i is the equivalent radius of the inner square cylinder (equal side length) and it is constant, and r_o is the equivalent radius of the outer elliptical enclosure and it is varied according to:

$$r_o = \frac{1}{\left(\cos(x)^{2n} + \sin(x)^{2n}\right)^{(1/2n)}} \ldots(8)$$

For the range of transformed computational domain to x and

h planes as $0 \le h \le 1$ and $0 \le x \le 2p$. A typical generated grid is show in **figure (2)** for 41×41 nodes.

The imposed boundary conditions are no slip and isothermal on both inner square cylinder and outer elliptical enclosure surfaces. Therefore, the boundary conditions could be express as:

$$y\big|_{h=0} = 0. \quad , \quad y\big|_{h=1} = 0.$$

$$T\big|_{h=0} = 1. \quad , \quad T\big|_{h=1} = 0.$$

$$w\big|_{h=0,1} = \frac{C}{J} \cdot y_{hh}\big|_{h=0,1} \ , \ y_h\big|_{h=0,1} = 0 \qquad \ldots.(9)$$

Numerical method

The governing equation in the curvilinear coordinates (equations 2, 3, and 4) as well as boundary conditions (equation 9) were discretized by finite difference method. Where equations 2, 3, 4, and 9, provide a complete description of the problem. In this study the finite difference equation were derived by using central difference approximation for the partial derivatives except the convective terms for which upwind difference formula was employed. Derivative at the boundary were approximated by three point forward or backward difference. The explicit method was chosed for the solution of flow and energy fields, while relaxation method was chose for stream function calculation. A time increment $\Delta t = 10^{-5}$ has been used for $Ra=10^3$-10^5 and 10^{-7} for $Ra=10^6$.

Additionally, the dimensionless local and average Nusselt number on the hot square cylinder has been calculated by the following expression [5]:

$$Nu_l = \frac{-1}{J \cdot \sqrt{a}} (a \cdot T_x - s \cdot T_h) \ldots(10)$$

$$Nu_{ave} = \frac{1}{2p} \int_0^{2p} Nu_l \cdot dx \qquad \ldots(11)$$

Grid Independency study

Several grids have been tested for the case of HEE, $Ra=10^5$, $a/b = 2.$, and $l/b = 0.25$. Table (1) shows the average Nusselt number for four grids used.

It can be see that, a little difference between the last two sets of grid results and the grid of 41×41 is used in all subsequent calculation of this study to decrease the time cost of the solution convergence, without effecting in the solution accuracy.

Validation Test

To validate the code validation, the natural convection problem for a low temperature outer square enclosure and high temperature inner circular cylinder was tested. The calculations of average Nusselt numbers for the test case are compared with the benchmarks values by Moukalled and Acharya **[8]** and Shu et. al **[9]** for different values of the aspect ratio L/D and Rayleigh number as given in table (2).

In addition, the validation test data of the streamline, isothermal contours compared with the results of Shu et. al **[9]** for $Ra=10^5$ and aspect ratios (L / D = 1.67) as shown in **figure (3)**, where L and D represented the side length of the outer square cylinder and the diameter of the inner circular cylinder respectively.

Results and Discussion

The results are presented for a number of cases (48 different physical domains) corresponding to two different cases, horizontal elliptical enclosure (HEE), and vertical elliptical enclosure (VEE), moreover to different geometric ratio a/b and l/b, and Rayleigh numbers. The basic features of flow and heat transfer are analyzed with the help of the velocity vectors, streamlines pattern, and isothermal contours. In addition, local Nusselt numbers on the hot isothermal surface of the inner square cylinder are plotted.

Flow pattern and heat transfer

For all Rayleigh numbers considered in this study, the flow and thermal fields eventually reach steady state with symmetric shape about the vertical centerline through the center of the square cylinder. Thus the present problem has a symmetry about the vertical centerline at $x = 0$. So, only one half of the geometry is chosen as the computational domain due to symmetry as shown in the results.

Figure (4) shows the velocity vectors, streamlines and isothermal contours for HEE case and $a/b = 2$, $l/b = 0.25$ for different values of Ra=10^3 to 10^6. In general, the flow behavior can be described as fellow: the hot square cylinder pumps the hot fluid in the domain and rises upward near the vertical mid plane of the elliptical enclosure (point P4) due to thermal expansion. This hot fluid moves with the path of elliptical enclosure wall after impinging on the roof. Finally, the colder and thus denser fluid descends along the cold sidewall as it meets cooled fluid a way from the cylinder.

From **figure (4)**, for low Ra, the heat transfer in the elliptical enclosure is mainly dominated by the conduction mode and the circulation of the flow shows one overall rotating eddy with one vortex as a circle shape according to the streamlines simulation due to the weakness in convection contribution. However, if Ra increases the role of convection in heat transfer becomes more significant and consequently the thermal boundary layer on the surface of the inner square cylinder becomes thinner. In addition, a plump starts to appear on the top of the square cylinder and as a result, the isotherms move upward giving rise to a strong thermal gradient in the upper region of the enclosure (from P3 to P4). Moreover, much lower thermal gradient in the lower region in the enclosure (from P1 to P2).

In consequence, the dominant can be see, flow is in the upper region of the enclosure, the vortex exists nearly in the middle of the enclosure, and its moves towards the upper region as Rayleigh number increase, where the flow at the lower region in the enclosure is very weak compare with that at the middle and top regions. The increase in Rayleigh number leads to deform the isotherms due to dissipated in the thermal boundary layer on the square cylinder from the bottom to the top and on the elliptical enclosure wall surface from the top to the bottom. Isothermal contours are uniform and regular for low Rayleigh number but as Ra increases these lines redistributed irregularly from hot square cylinder to the elliptical enclosure due to the higher in convection contribution.

If the l/b ratio increases, the thermal mixing of the flow will be strong and the isothermal contours could be more deform from the previous case, as shown in **figure (5)** for $l/b = 0.5$. As it can be seen from this figure for high Rayleigh number, there are two vortices in the domain especially at Ra $\geq 10^5$ because the source of the heat region is large compared with the previous case (figure 4).

The same behavior of flow pattern and isothermal contours could be see at **figures (6)**, and **(7)** for vertical elliptical enclosure case (VEE), but the flow is weak comparing with that at (HEE) case due to a smaller flow domain thus smaller flow strength (streamlines value) especially at low Rayleigh number. In **figure (6)** the flow is compressed in the domain and one vortex exits nearly in the middle of the domain at low Rayleigh number, but if Ra increases this vortex moves up to the upper region of the enclosure and its becomes greater than of that in low Rayleigh number. Isothermal contours for VEE case as shown in **figure (6)** have the same behavior of HEE case but for different values of temperature, where it uniform for low Ra and non uniform, with more deformation for high Ra, due to the change in the thermal boundary layer.

If the ratio l/b increases as shown in **figure (7)** three vortices located in the on the upper, middle, and lower regions in the enclosure are developed for low Ra, but if Ra increases the middle and lower vortices are finished and the upper vortex is become larger and deform downward the enclosure.

Effect of The Geometric Parametes

In order to asses the effect of the geometric parameters a/b and l/b ratios, three different configurations a/b =1.5, 2, and 3, and two ratio of l/b =0.25, and 0.5 have been studied in the present study for two cases of (HEE), and (VEE).

Figure (8) demonstrates the case of (HEE), Ra=10^6, and l/b =0.25, if a/b ratio increase the streamline extended towards the major axis of the elliptical enclosure, and the isothermal contours values decreases. In addition, the thermal flux dissipated towards the major axis and weakened at the lower region of the enclosure. For l/b ratio, as it is increased as shown in **figure (9)** leads to two vortices in the enclosure, first vortex located at the upper region of the enclosure while the second vortex located at the middle of the domain close to the upper cold surface. Moreover, if the a/b ratio increases the vortices in the domain become weak and small due to the heat removal from the square cylinder. Isothermal contours also become weak with increase a/b ratio.

Figure (10) and **(11)** show the results of local Nusselt number on the hot square cylinder surface for different conditions of a/b, l/b ratios and Rayleigh number for two cases of enclosure position (HEE, VEE). **Figure (10)** shows that for (HEE) case, where for all values of Rayleigh number (A, B, and C) the curves growth gradually from lower value of Nu_l at the point P1 at the lower surface of the square cylinder due to small temperature difference

in this region (weak thermal boundary layer). Moreover, suddenly, could be take a first peak value at the lower tip of the square cylinder at point P2 due to the sudden change in the surface geometry and to increase in the temperature difference. The Nu_l increases gradually due to growth of thermal boundary layer in the middle of the elliptical enclosure especially at high Rayleigh number, so, the temperature difference increases too, until reach to the second peak value at the point P3, due to the change of the surface geometry. After point P3 the thermal boundary layer could be reduced and leads to a temperature difference in this region comparing with that before point P3. Also, **figure (10)** (A, B, and C), show that as a/b ratio increase leads to increase in the value of Nu_l for all cases of Rayleigh number due to extended in the major axis of the elliptical enclosure (enclosure become wider), moreover to the increase in the temperature difference according to that.

The right side of **figure (10)** (D, E, and F) for case $l/b=0.5$, clarified nearly the same behavior with different values of Nu_l except at high Rayleigh number Ra=10^6, where there is a decrease in the Nu_l in the lower region of the enclosure (from P1 to P2) due to the creation of two eddies vortices in the domain resulted from strong thermal boundary layer. After point P2 the curves have the same behavior as shown in the previous figures (A, B, and C) with different values of local Nusselt number, also, increase a/b ratio leads to increase the peaks values of the curve of Nu_l for all Rayleigh numbers. Also, If l/b ratio increase leads to decrease in the values of Nu_l at fixed values of a/b ratio for all Rayleigh numbers with change in the behavior in Ra=10^6 case, due to the creation of two eddy vortices in the domain for higher l/b ratio and for strong thermal boundary layer in this case.

Figure (11) indicates the local Nusselt number on the hot surface of square cylinder for different ratios of a/b, l/b ratios and Rayleigh number for (VEE) case. The same behaviors could be see as shown in previous figure with different values of Nu_l, except at Ra=10^6, $l/b=0.5$, HEE, where there are two vortices in the domain and changed in the profile. Where increasing a/b ratio leads to increase the peaks values of the curve of Nu_l at fixed l/b ratio for all Rayleigh numbers values. Also increase l/b ratio leads to decrease Nu_l at fixed a/b ratio for all Ra. Also for fixed case, the Nu_l in (VEE) case is greater than to that at (HEE) case.

Tables (3), and (4) show the values of the flow strength and average Nusselt number for different ratios of a/b, l/b and Rayleigh number for (HEE) and (VEE) cases. From the results, increasing Rayleigh number leads to increase values of flow strength and Nu_{ave} due to the increasing effect of convection. Also for fixed Rayleigh number, increasing a/b ratio leads to decrease in flow strength and increase in the values of Nu_{ave} for both cases of HEE and VEE. Also,

increase the l/b ratio leads to decrease in the flow strength at Ra$\leq 10^4$ in HEE case and at Ra$\leq 10^5$ in VEE case, otherwise the flow strength increase, and decrease in Nu_{ave} for both cases. Moreover, it was found that, the position of the major axis of the elliptical enclosure (HEE, and VEE cases) has noticeable large effect on the streamlines, and very little effect on the average Nusselt number.

Conclusions

The present study investigates numerically the flow and heat transfer characteristics of a two-dimensional natural convection problem on a hot square cylinder placed in a cooled ellipticall enclosure. A detailed analysis for the distribution of streamlines, isotherms and Nusselt numbers were carried out to investigate the effect of the position of the major axis of the enclosure for two cases HEE, and VEE, with different geometric parameters a/b, and l/b on the flow field and heat transfer in the enclosure for different Rayleigh number in the rang 10^3 to 10^6. For all Rayleigh numbers considered in the present study the flow and thermal fields eventually reach the steady state with the symmetric shape about the vertical centerline of the enclosure. The major results may be summarized as follows: **(1)** At fixed a/b, l/b ratios, the average Nusselt number increase with increase in Rayleigh number; **(2)** The increase of major axis of the enclosure (a/b ratio) leads to increase the average Nusselt number and decrease the flow strength for all Rayleigh number; **(3)** For Ra$\leq 10^4$, there are a little difference in the results of Nu_{ave} for all a/b and l/b ratios, but if Ra increase, the change in the results could be clear and large; **(4)** Increase the l/b ratio leads to decrease in the flow strength at Ra$\leq 10^4$ in HEE case and at Ra$\leq 10^5$ in VEE case, otherwise, the flow strength increase, and decrease in Nu_{ave} for both cases; **(5)** In HEE, and VEE cases there are little change in the values of the Nu_{ave}, with large difference in the flow strength.

Nomenclature

A,B,C, G, H	Transformation parameters.
a, b	Half of the major and the minor axis length respectively (m)
J	Jacobian
l	Side length of the square cylinder (m)
Nu	Nusselt number
P1,P2 P3,P4	Points on the square cylinder surface
Pr	Prandlt number
Ra	Rayleigh number
T	Dimensionless Temperature
g	Gravitational acceleration (m/sec^2)
HEE, VEE	Horizontal, and Vertical elliptical enclosure
u , v	Dimensionless contravariant velocity components in ξ, and η coordinates
x, y	Dimensionless Cartesian coordinates

Greek symbols

α, γ, σ	Transformation functions
β^*	Thermal expansion coefficient (1/k)
α^*	Thermal diffusivity of fluid (m^2/sec)
ξ , η	curvilinear coordinates

y	Stream function
w	Vorticity
ν	Kinematics viscosity (m^2/sec)
∇^2	Operator Laplace

Superscripts

$\bullet$	Dimensional form

Subscripts

ave	Average
c	Cold surface
h	Hot surface
l	Local
max	Maximum value
x, y	Derivative relative to
x, h, t	$x, y, x,$ and h respectively.

References

[1] Ding, H., Shu, C., Yeo, K.S., and Lu, Z.L., "***Simulation of a natural convection in eccentric annuli between a square outer cylinder and a circular inner cylinder using local MQ-ΔQ method***'", Numer. Heat Transfer, part A, 47, 2005, pp. (291-313).

[2] Shu, C., Xue, H., and Zhu, Y.D., "***Numerical study of natural convection in an eccentric annulus between a square outer cylinder and a circular inner cylinder using DQ method***", Int. J. of heat and mass transfer**,** 44, 2001, pp. (3321-3331).

[3] Roychowdhury, D.G., Das, S.K., and Sundararajan, T.S., "***Numerical simulation of natural convection heat transfer and fluid flow around a heat cylinder inside an enclosure***", J. of heat and mass transfer**,** 38, 2002, pp. (565-576).

[4] Asan, H., "***Natural convection in an annulus between two isothermal concentric square ducts***", Int. comm.. heat mass transfer, 27, 2000**,** pp. (367-376).

[5] Kumar De, A., and Dalal, A., "***A numerical study of natural convection around a square horizontal heated cylinder placed in an enclosure***", Int. J. heat mass transfer, 49, 2006, pp. (4608-4623).

[6] Kim, B.S., Lee, D.S., Ha, M.Y., and Yoon, H.S., "***A numerical study of natural convection in a square enclosure with a circular cylinder at different vertical locations***", Int. J. heat and mass transfer, 51, 2008, pp. (1888-1906).

[7] Cesini, G., Paroncini, M., Cortella, G., and Manzan, M., "***Natural convection from a horizontal cylinder in a rectangular cavity***", Int. J. heat mass transfer, 42, 1999, pp. (1801-1811).

[8] Moukalled, F., and Acharya S., "***Natural convection in the annulus between concentric horizontal circular and square cylinders***", J. Thermophys. Heat transfer, 10, 1996, pp. (524-531).

[9] Shu, C., and Zhu, Y.D., "***Efficient computational of natural convection in a concentric annulus between an outer square cylinder and inner circular cylinder***", Int. J. Numer. Meth. Fluid, 38, 2002, pp. (429-445).

[10] Tasnim, S. H., and Mahmud, S., "***Laminar free convection inside an inclined L-shaped enclosure***", Int. J. heat and mass transfer, 33, 2006, pp.

(936-942).

[11] Zhu, Y. D., Shu, C., Qiu, J., and Tani, J., " ***Numerical simulation of natural convection between two elliptical cylinders using DQ method***", Int. J. heat and mass transfer, 47, 2004, pp. (797-808).

[12] Shu, C., "***Differential quadrature and its application in engineering***",Springer-Verlag, London, 2000.

[13] Baehr, H. D., and Stephan, K.," ***Heat and mass transfer***," second, revised edition, Springer-Verlag, Germany, 2006.

[14] Thompson, J. F., soni, B.K., and weatherill, N. P., "***Handbook of grid generation*", ** New York, by CRC Press LLC, 1999.

Table 1 Nu_{ave} results for several grids for HEE, Ra=10^5, $a/b=2.$, and $l/b=0.25$

Grid size	Nu_{ave}	$\lvert y_{max} \rvert$
21×21	9.89	11.88
31×31	10.42	12.03
41×41	10.63	12.44
51×51	10.64	12.46

Table 2 Comparison of the present average Nusselt number with those of the previous studies of references [8] and [9].

L / D	Ra	[8]	[9]	Present study
5	10^4	2.071	2.08	2.105
2.5		3.331	3.24	3.195
1.67		5.826	5.40	5.413
5	10^5	3.825	3.79	3.807
2.5		5.080	4.86	5.050
1.67		6.212	6.21	6.182
5	10^6	6.107	6.11	6.201
2.5		9.374	8.90	9.254
1.67		11.62	12.0	11.624

Table (3) Flow strength and average Nusselt number for HEE case

$\frac{a}{b}$	Ra	$\lvert y_{max} \rvert$		Nu_{ave}	
		$l/b =$			
		0.25	**0.5**	**0.25**	**0.5**
1.5	10^3	0.868	0.563	3.612	3.606
2		0.624	0.506	4.586	4.470
3		0.290	0.268	6.692	6.436
1.5	10^4	5.639	4.379	5.070	4.090
2		4.465	3.938	5.984	5.068
3		2.562	2.394	7.592	6.788
1.5	10^5	14.17	14.61	8.991	6.291
2		12.44	13.93	10.63	7.623
3		9.29	9.787	13.38	9.503
1.5	10^6	27.84	28.41	15.53	12.50
2		23.89	24.76	18.60	14.89
3		18.88	21.14	23.41	18.27

Table (4) Flow strength and average Nusselt number for VEE case

$\frac{a}{b}$	Ra	$\lvert y_{max} \rvert$		Nu_{ave}	
		$l/b =$			
		0.25	**0.5**	**0.25**	**0.5**
1.5	10^3	0.35	0.11	3.494	3.458
2		0.185	0.079	4.417	4.404
3		0.081	0.040	6.213	6.209
1.5	10^4	3.528	1.377	4.624	3.652
2		2.007	1.019	5.115	4.463
3		0.832	0.452	6.447	6.223
1.5	10^5	15.50	10.63	9.146	5.694
2		13.00	9.474	10.76	6.382
3		7.94	5.738	12.60	7.950
1.5	10^6	29.69	33.01	15.77	10.65
2		28.11	31.95	19.32	13.03
3		28.06	30.72	25.25	16.87

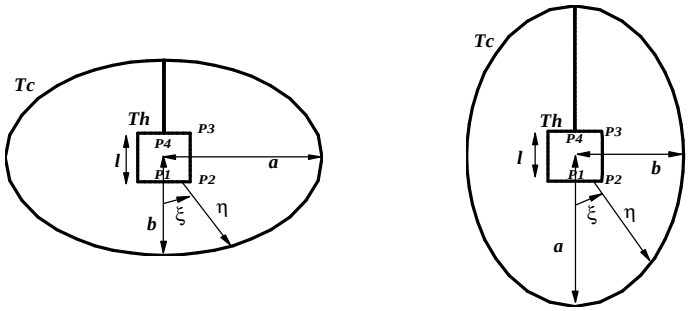

Figure (1) A schematic view and geometry description of the physical domain Left side: HEE right side: VEE

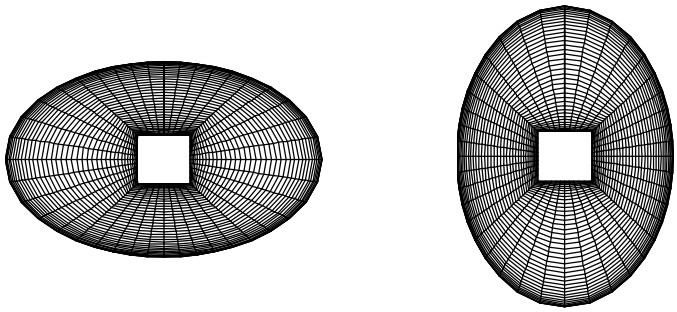

Figure (2) A typical grid generation (41*41 grids) for $a/b=1.5$, $l/b=0.25$ Left side: HEE right side: VEE

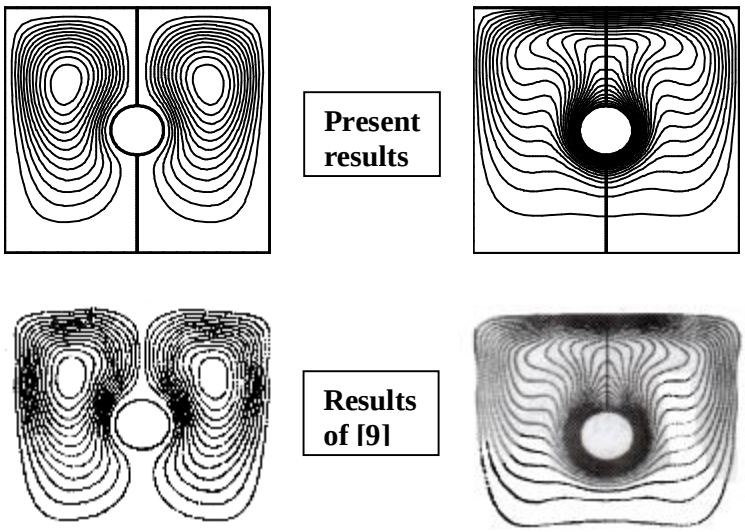

Figure (3) A comparison of the present results with that of reference [9] for $Ra=10^5$, and L/D=1.67, Left side: Streamlines right side: isotherms

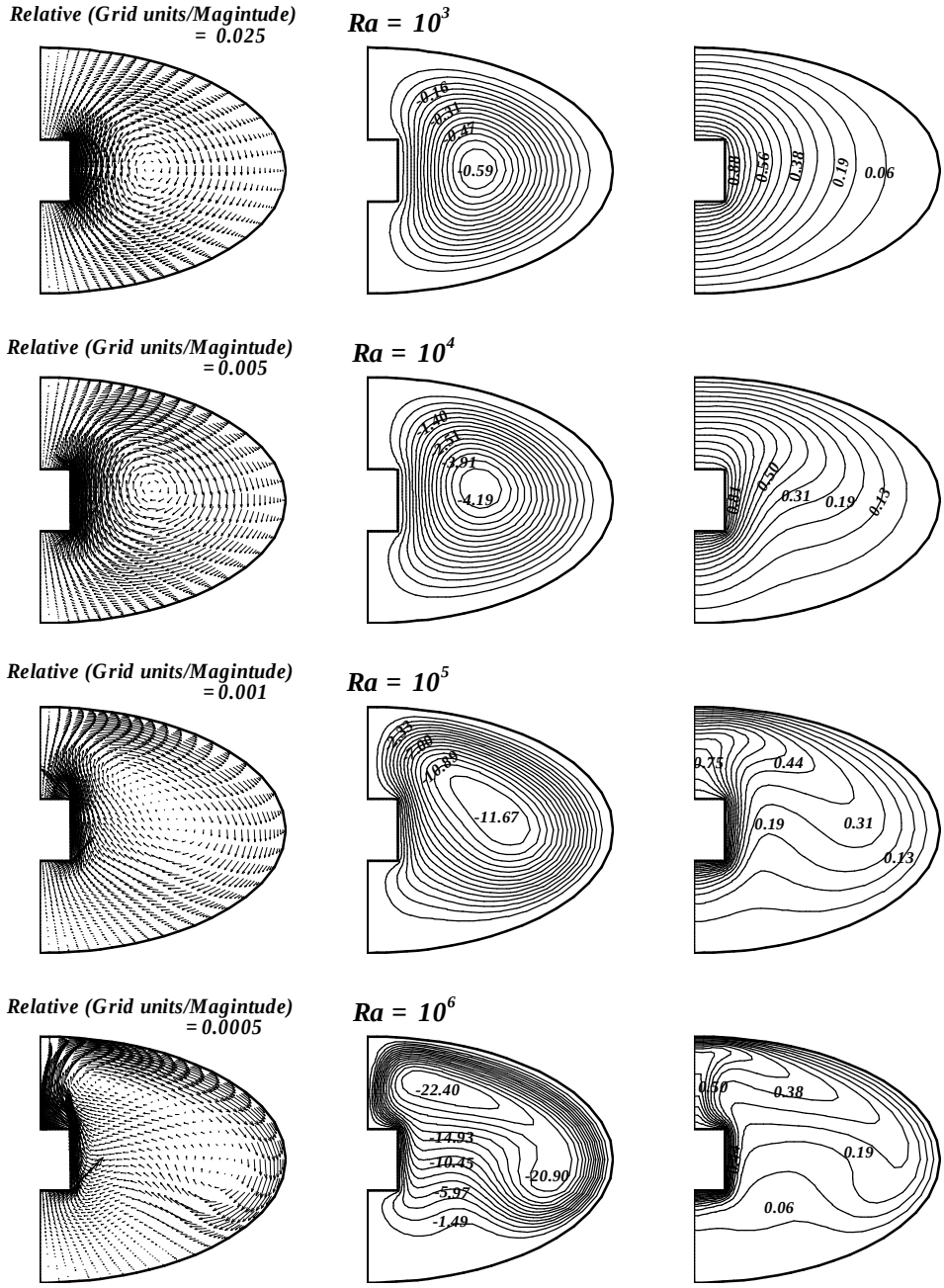

Figure (4) Velocity vectors (left side), streamlines (middle side), and isotherms (right side) for $a/b = 2, l/b = 0.25$**, and HEE case.**

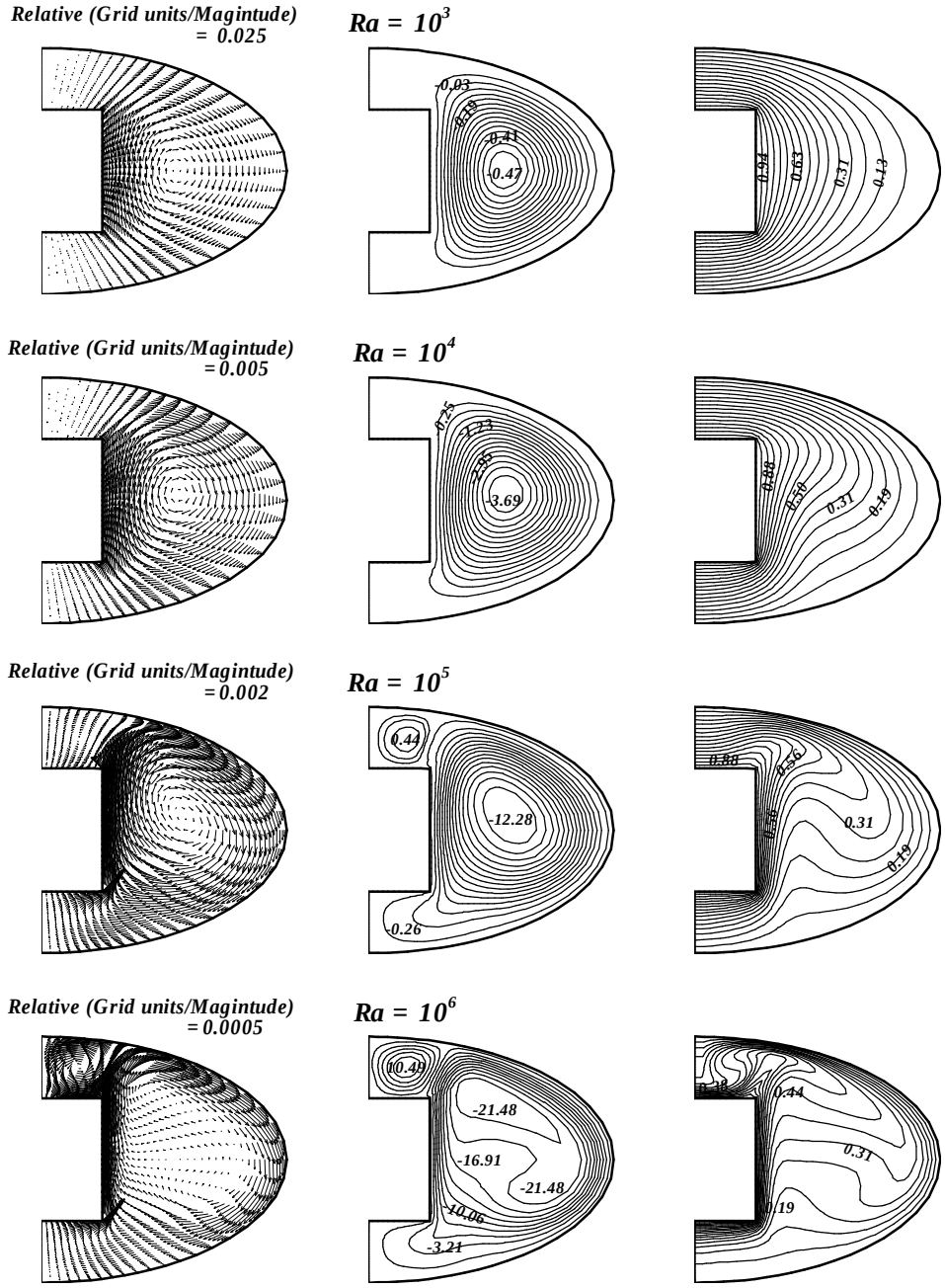

Figure (5) Velocity vectors (left side), streamlines (middle side), and isotherms (right side) for $a/b = 2, l/b = 0.5$, and HEE case.

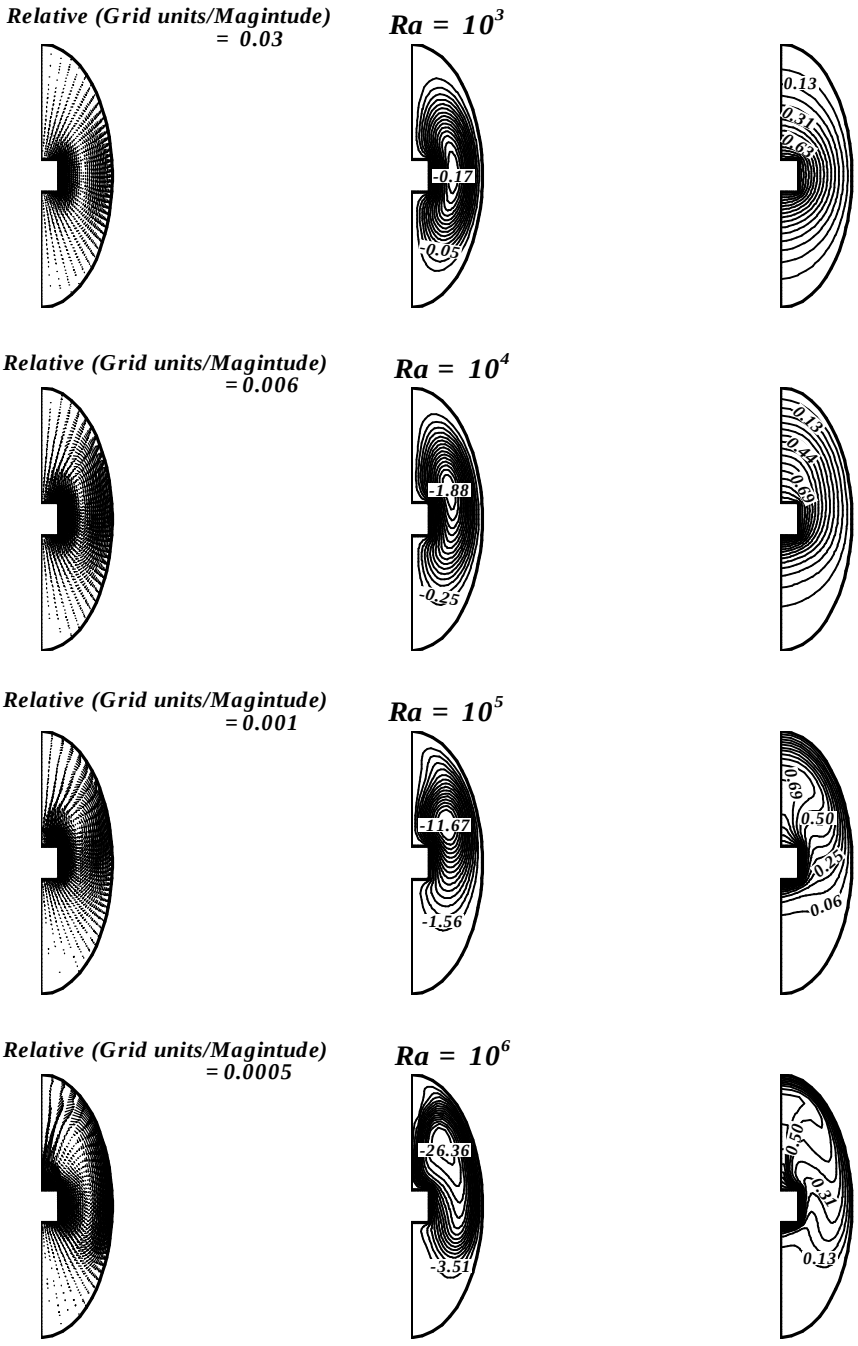

Figure (6) Velocity vectors (left side), streamlines (middle side), and isotherms (right side) for $a/b = 2, l/b = 0.25$**, and VEE case.**

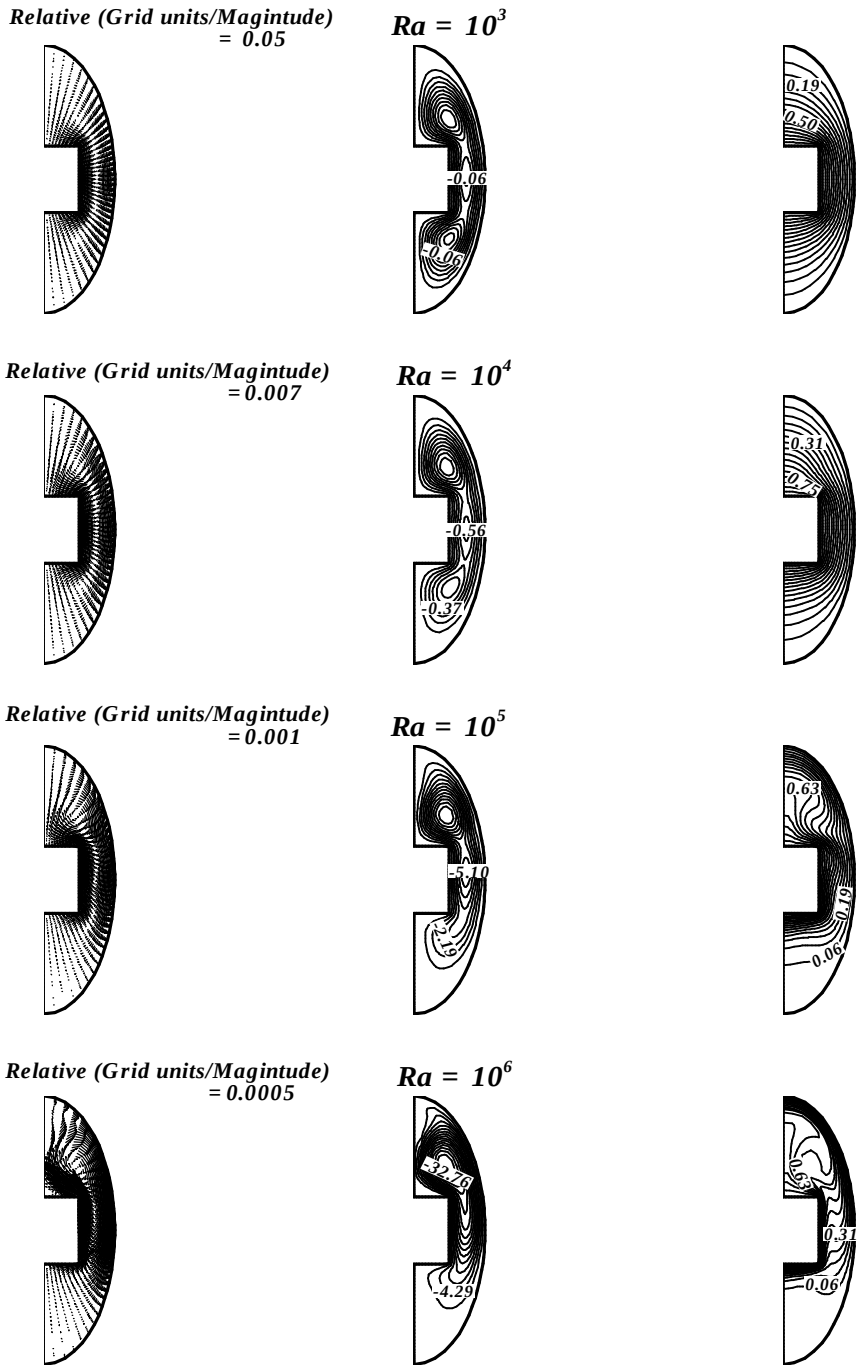

Figure (7) Velocity vectors (left side), streamlines (middle side), and isotherms (right side) for $a/b = 2, l/b = 0.5$ **, and VEE case.**

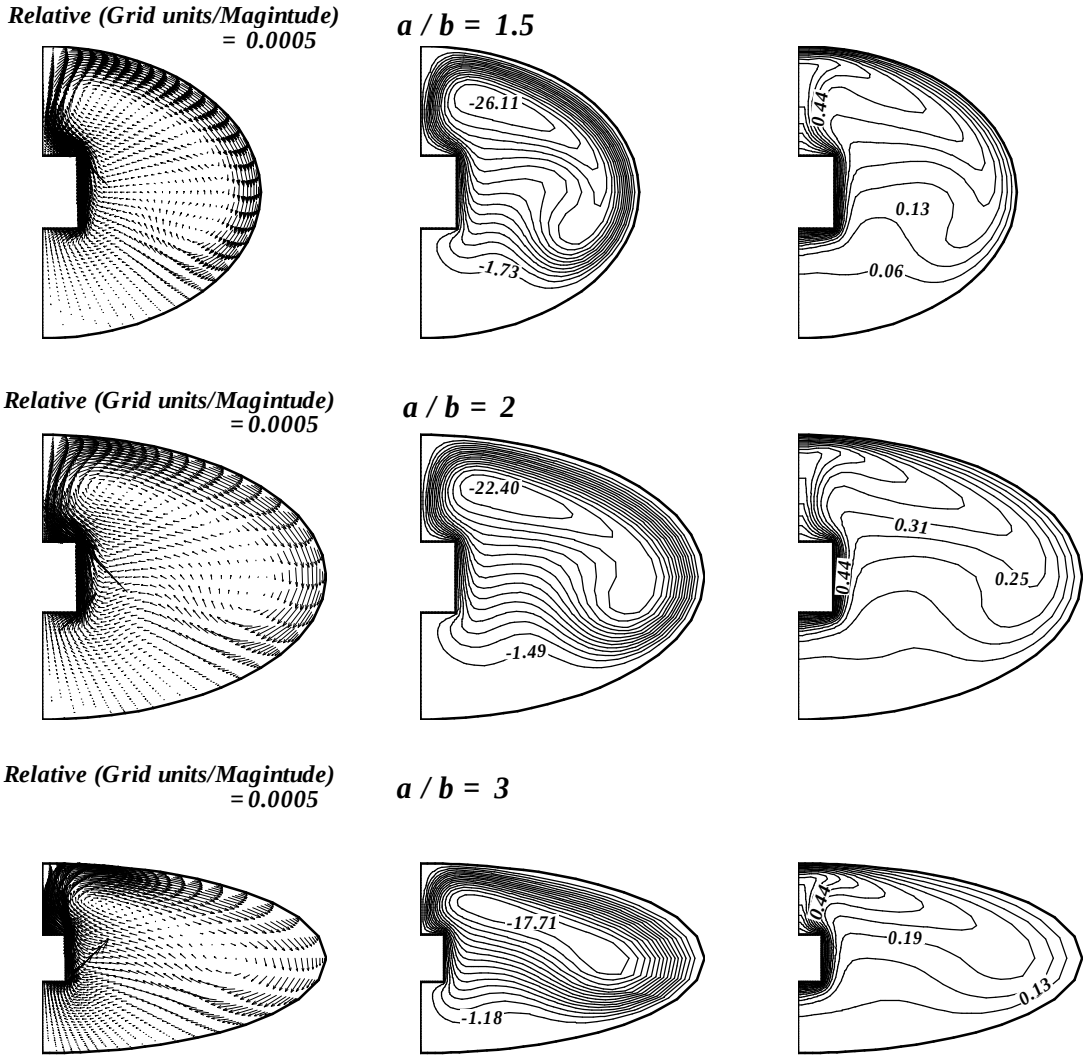

Figure (8) Velocity vectors (left side), streamlines (middle side), and isotherms (right side) for different a/b ratio, and $Ra=10^6$, $l/b = 0.25$, HEE case.

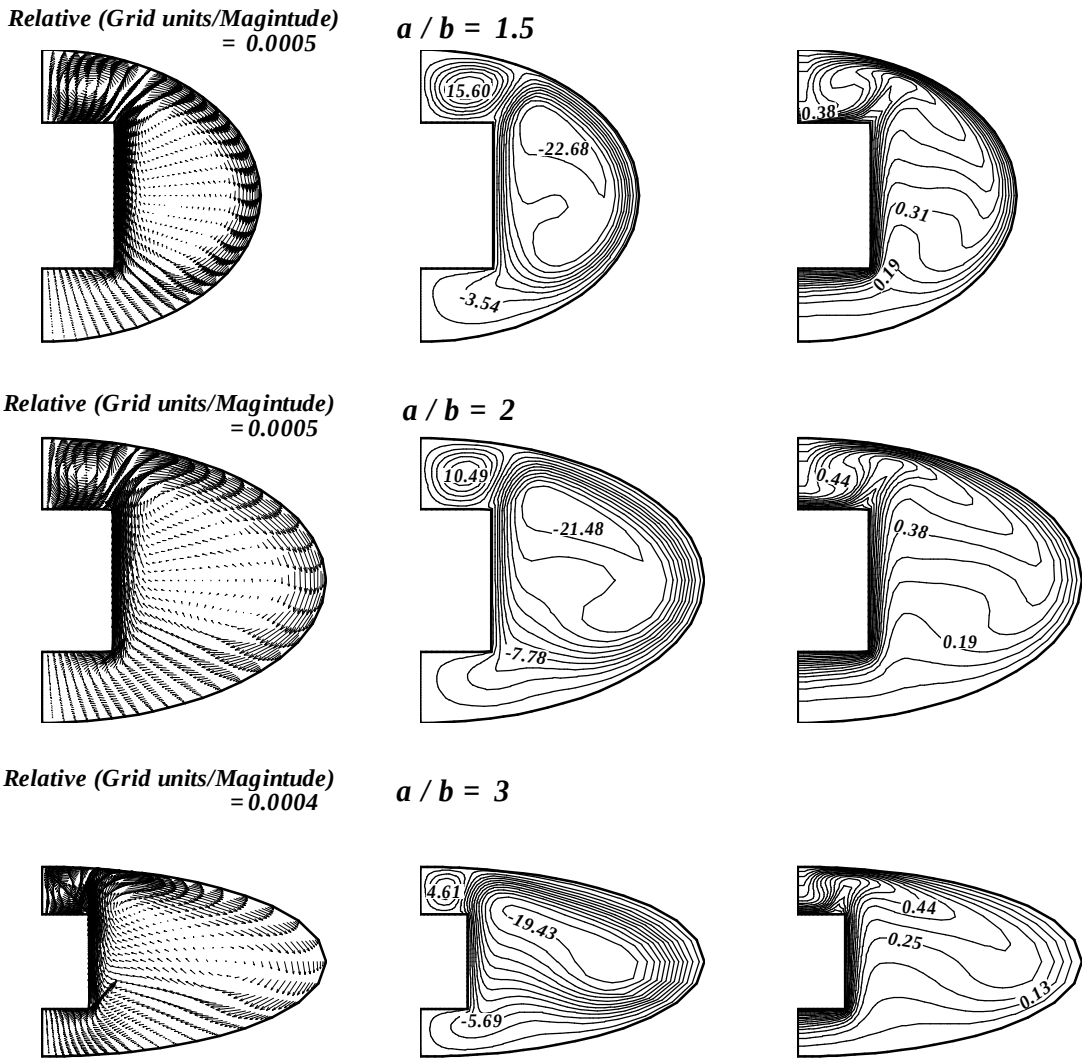

Figure (9) Velocity vectors (left side), streamlines (middle side), and isotherms (right side) for different a/b ratio, and $Ra=10^6$, $l/b=0.5$, HEE case.

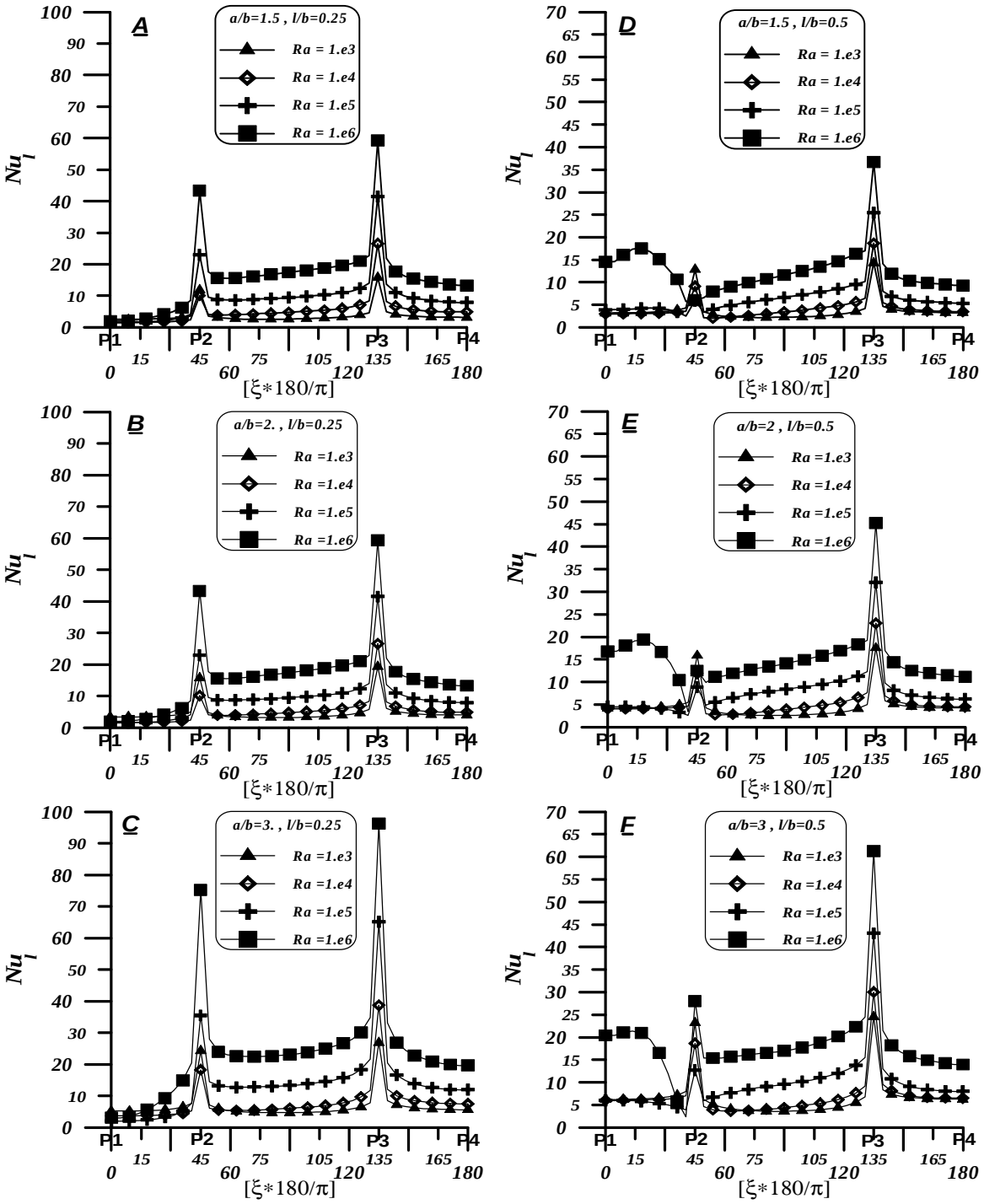

Figure (10) Local Nusselt number distribution on the hot square cylinder surface for different geometric parameters (a/b , l/b), and different Rayleigh numbers in HEE case.

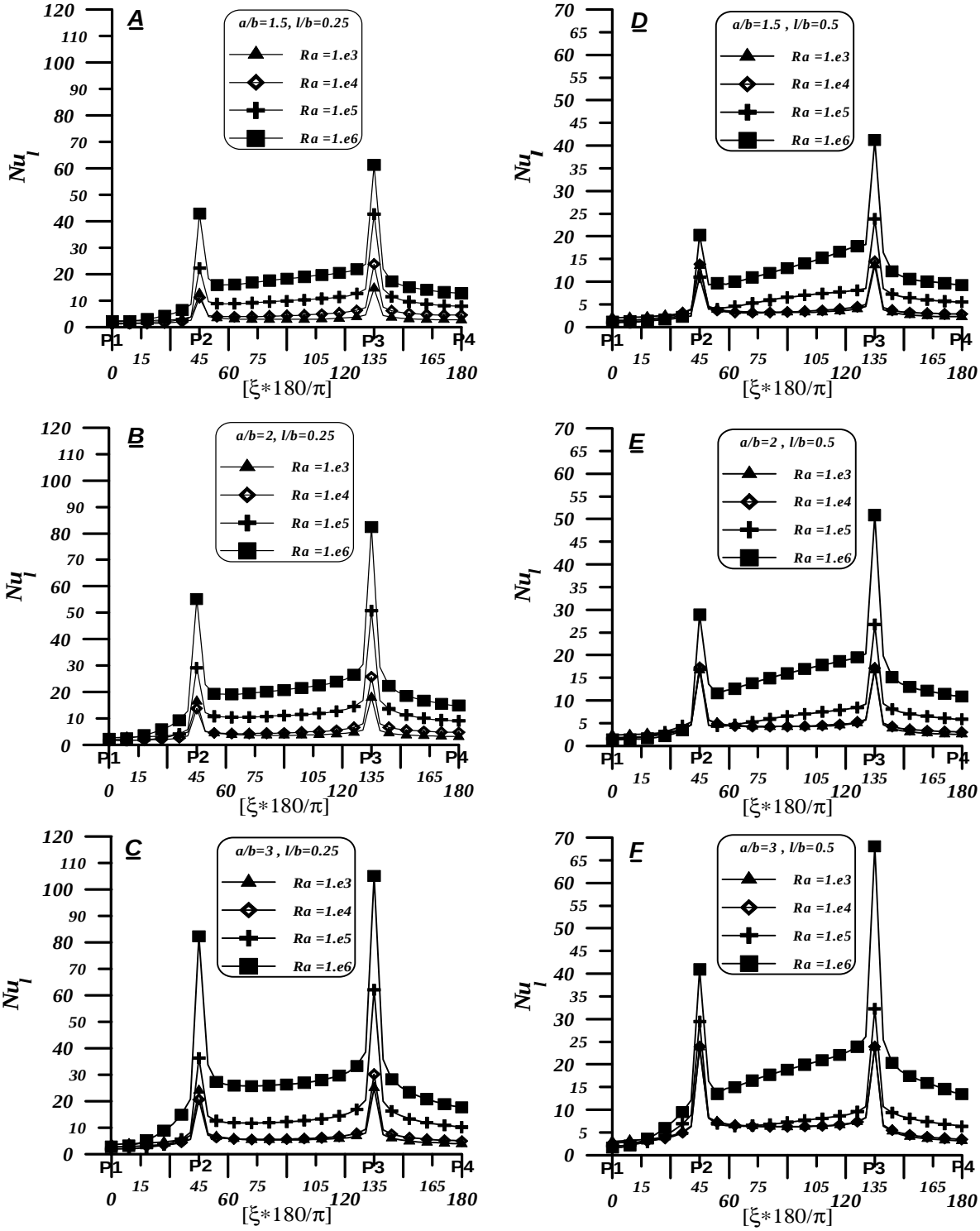

Figure (11) Local Nusselt number distribution on the hot square cylinder surface for different geometric parameters (a/b , l/b), and different Rayleigh numbers in VEE case.